THE GREAT WORLD OF NANOTECHNOLOGY

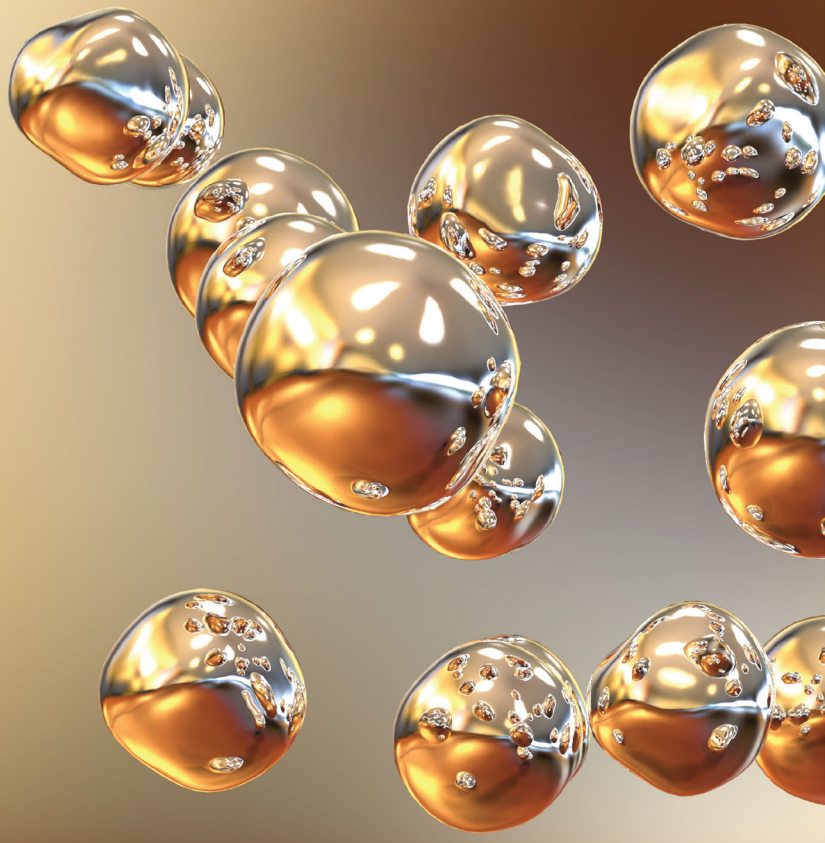

Marcos Augusto de Lima Nobre

(Organizador)

VOL II

EDITORA ARTEMIS
2021

THE GREAT WORLD OF NANOTECHNOLOGY

Marcos Augusto de Lima Nobre

(Organizador)

VOL II

EDITORA ARTEMIS
2021

Editora Chefe Profª Drª Antonella Carvalho de Oliveira
Editora Executiva M.ª Viviane Carvalho Mocellin
Direção de Arte M.ª Bruna Bejarano
Diagramação Elisangela Abreu
Organizadoras Prof. Dr. Marcos Augusto de Lima Nobre
Imagem da Capa Kateryna Kon
Bibliotecário Maurício Amormino Júnior – CRB6/2422

Editora Artemis
Curitiba-PR Brasil
www.editoraartemis.com.br
e-mail:publicar@editoraartemis.com.br

Dados Internacionais de Catalogação na Publicação (CIP)
(eDOC BRASIL, Belo Horizonte/MG)

G786 The great world of nanotechnology [livro eletrônico] : vol. II /
Organizador Marcos Augusto de Lima Nobre. – Curitiba, PR: Artemis, 2021.

Formato: PDF
Requisitos de sistema: Adobe Acrobat Reader
Modo de acesso: World Wide Web
Inclui bibliografia
Edição bilíngue
ISBN 978-65-87396-36-1
DOI 10.37572/EdArt_300621361

1. Nanociência. 2. Nanotecnologia. I. Nobre, Marcos Augusto Lima.

CDD 620.5

Elaborado por Maurício Amormino Júnior – CRB6/2422

EDITORA ARTEMIS
2021

Editora Artemis
Curitiba-PR Brasil
www.editoraartemis.com.br
e-mail:publicar@editoraartemis.com.br

PREFACE

The insertion of new and enhanced materials based on materials belonging to the Nano scale in the day-by-day has growth up in a silent way. In part, a number of works in the nanotechnology stemming of theoretical research using Density Functional Theory (DFT) and sophisticated simulation methods; another part is associated to the protected technologies associated to the military and patented nanomaterial and its process. In this sense, open access to recent aspects on the nanostructures application and properties can be reached in this book. Here, an interesting set of chapters gives opportunity of access texts that reach process and processing of nanostructures, applications of nanotechnology, advanced techniques to theoretical development. A broad set of nanostructures are here covered such as, nanocrystal, superficial nanograins, inner microstructures with nanograins, nanoaggregates, nanoshells, nanotubes, nanoflowers, nanoroad, nanosheets, Also, reveals new investigations areas as grainboundary of nanograins in ceramics and metals. A great number of software has been used as a tool of development of Science and Technologies for nanotechnology COMSOL Multiphysics 5.2. Phenomena and properties has been investigated by recent or classical techniques of materials characterization as Localized Surface Plasmon Resonance (LSPR), X-ray photoelectron spectroscopy (XPS), Field Emission Gun Scanning Electron Microscopy (FEG-SEM) with Energy Dispersive Spectroscopy (EDS), Raman Scattering Spectroscopy (RSS), X ray diffraction (XRD), ^{57}Fe Mössbauer spectroscopy, UV-vis spectroscopy, dynamic light scattering (DLS), Atomic Force Microscopy (AFM), and Field Emission Gun Scanning Electron Microscopy (FEG-SEM). In this sense, collections of spectra from Mössbauer spectroscopy, UV-vis spectroscopy and Infrared spectroscopy can be found. As a matter of fact, some chapter's item can be seemed as specific protocols for synthesis, preparations and measurements in the nanotechnology.

I hope you enjoy your reading.

Prof. Dr. Marcos Augusto Lima Nobre

TABLE OF CONTENTS

CHAPTER 3

AB-INITIO STUDY OF ELECTRONIC AND MAGNETIC PROPERTIES OF ZnO NANOCRYSTALS CAPPED WITH ORGANIC MOLECULES

Data de submissão: 07/04/2021
Data de aceite: 29/04/2021

Aline L. Schoenhalz
Federal University of Santa Maria
Physics Department
Santa Maria – RS
http://lattes.cnpq.br/2996035802901172

Paulo Piquini
Federal University of Santa Maria
Physics Department
Santa Maria – RS
http://lattes.cnpq.br/4496249071363237

ABSTRACT: Unexpected ferromagnetic ordering in nonmagnetic metal oxide nanostructures, such as ZnO nanoparticles, has been attributed to several controversial origins. The experimental determination of the ZnO nanoparticle properties is difficult by the diminutive and the possible conformational, and chemical complexity of the systems. Systematic reliable theoretical studies using first principles density functional theory calculations have been applied to study the structural, electronic, energetic and magnetic properties of ZnO nanocrystals both pristine and bonded to thiol, amine and TOPO organic ligands. Our results show that the capping of ZnO nanocrystals by different organic molecules induces electronic and structural transformations that directly affect their magnetic behavior. It is shown that structural distortions resulting from the interactions between the organic molecules and the surface layers is one of the main factors to reducing the total magnetic moment of the capped ZnO nanoparticles.
KEYWORDS: ZnO nanocrystals. DFT. Nanostructures surface.

1 INTRODUCTION

Nanostructures surface chemistry is a very rich an ample field of research, where semiconductor and metallic quantum dots have a prominent position. Most of these systems have their sizes reduced to few nanometers, i.e., the same order or smaller than the bulk exciton Bohr radius. At this scale, quantum confinement and surface effects are significant and the electronic and optical properties will deviate considerably from those of their bulk counterparts.

The surface of these nanomaterials presents, in general, many different structural patterns. The surface atoms are usually undercoordinated and chemically different from those at the core. These dangling bonds

can promote a structural disorder at nanostructures surface as well as originate trapping charge states within their energy bandgap (AZPIROZ et al., 2015; SINGLA et al., 2009; GUGLIERI et al., 2012) Possibilities to remediate this issue involve the incorporation of inorganic shells, such as CdSe, CdTe and ZnS (WANG et al., 2010; KIM et al., 2003; TALAPIN et al., 2001), or attaching organic molecules on the surface of the nanoparticle (HINES et al., 2014).

In fact, nanoparticle surfaces are, in general, very complex, presenting unbonded orbitals, reconstructions, intrinsic defects and impurities, and bonds to ligands (TSUI et al., 2016; VOZNYY, 2011). Unpaired electrons at the nanoparticle surfaces lead to highly reactive and energetically unfavorable sites. The passivation with organic ligands (also referred to as surfactants or capping agents) is of particular interest since this is a common method used to stabilize nanoparticle's surface, control the growth of some of their facets and modulate their optical properties (SINGLA et al., 2009; CHEN et al., 2016; NOH et al., 2019; GAO et al., 2019). The control of size, structure, and composition of nanoparticle surfaces can, in this sense, be explored to tune the material properties in order to have specific functionalities. Therefore, a suitable choice of the organic capping agents is crucial.

In case of semiconductors quantum dots and nanocrystals, such as CdSe, ZnS, ZnO among others, surfactants from the families of thiol, amine or phosphine are often used. The physical properties of the resulting nanonoparticle (nanocrystal+capping agent) will differ, depending on the choice of the adsorbed surfactant.

The magnetic response of organic-capped oxide-nanostructures is strongly dependent on the preparation conditions. For instance, capped ZnO nanoparticles are reported to have room temperature (RT) ferromagnetism in some experiments (GARCIA et al., 2007; GHOUL et al., 2020; BOUOUDINA, 2017; SAMANTA et al., 2018), while in others no ferromagnetism was detected (KITTILSTVED, et al., 2005). These controversial results show that even small structural/electronic variations can give rise to remarkable modifications in the magnetic properties of these materials.

The use of thiol molecules as capping agents is seen to enhance the optical properties of core-shell CdSe/ZnS QDs (ZHU et al., 2014). Further, the fluorescence quantum yields of CdSe and CdTe nanocrystals is observed to be greatly influenced by the capping of their surfaces with thiol molecules (WUISTER et al., 2004).

The TOPO molecule is known to weakly bind semiconductor surfaces like CdSe (KOPPING et al., 2008). This makes this capping agent very useful in processes where a previously QD+TOPO film is photobleached with UV irradiation under patterned masks, in order to obtain QD nets in a QD+TOPO film (PARK et al., 2011).

Actually, considerable advances have been made regarding quantum confinement effects in semiconducting nanostructures, but a precise description of phenomena taking place at these surface is still missing (HINES et al., 2014; YU et al., 2006; KUZNETSOV et al., 2014; SPERLING et al., 2010; KANGOA et al., 2013). Despite the importance of surface morphology and chemistry to the electronic and optical properties, much has to be known about the atomistic description of the passivation of semiconducting nanoparticles.

One case to be highlighted is the pristine ZnO nanoparticles. When the surface of this nanoparticle is passivated with amine, thiol and TOPO, different intensities of the magnetic response are observed. It is suggested that the surface rearrangement and the different passivation are the main influences to the detected magnetic behavior. In this work we explore, via first-principles simulations, the effects of the organic ligands such as thiol, amine and TOPO groups in the physical properties of ZnO nanocrystals, specially the trends in the structural, electronic and magnetic properties. Our results show that thiol and amine ligands have similar bonding properties. The TOPO ligands, on the other hand, are weakly bond and promote greater structural disorder on the ZnO surface layers. It is shown that the total magnetization will be critically dependent on the amount of passivation of the reactive sites, and on the resulting structural distortions at the ZnO surface layers.

2 COMPUTATIONAL METHODS

All calculations are performed using Density Functional Theory (DFT) (HOHENBERG et al., 1964) as implemented in the Vienna Ab-initio Package (VASP) (KRESSE et al., 1996). The Bloch functions are represented through the projected augmented wave method (PAW) (BLOCHL, 1994), with a plane-wave cutoff of 400 eV. The Perdew-Burke-Ernzerhof (PBE) (PERDEW et al., 1997) version of the generalized gradient approximation (GGA) was used to describe the exchange-correlation interactions. The GGA/PBE approach to DFT has been shown to correctly describe the adsorption of adatoms and molecules in nanostructures' surfaces (TANG et al., 2015; YU et al., 2015; CHABAN et al., 2013; BHATTACHARYA et al., 2008). Before the evaluation of physical properties, all structures were geometrically relaxed until the force components converge below 25 meV/Å. An additional single-point total energy calculation was done using the optimized structures and the PBE0 (ADAMO et al., 1999) hybrid functional in order to improve the electronic description of the systems. Repeated structures are separated by vacuum layers of at least 7 Å to avoid interactions between neighboring images.

The ZnO nanoparticle consists of a spherical cut of a zinc blende ZnO bulk, with a diameter of ~ 0.9 nm, having a Zn atom at its center, as represented in Fig. 1(a). The

bulk-like local geometry is maintained after structural optimization, although some small changes in bond angles can occur. This system, like other nanostructured semiconducting oxides, presents a magnetization without magnetic impurities (OSORIO-GUILLEN et al., 2006; SCHOENHALZ et al., 2009; PODILA, et al., 2010). This “crude” model has many broken bonds and consequently, reactive sites at its surface.

3 RESULTS AND DISCUSSION

The modelling of organic ligands on nanoparticle surfaces is a complicated subject due to the structural complexity and the several possible binding sites and geometries. The most probable reactive sites for the attachment of organic ligands on the ZnO nanoparticle surface were found through the calculation of the electrophilic and nucleophilic Fukui functions associated with this system (PARR et al., 1989; ALLISON et al., 2013).

The electrophilic sites, which are prone to receive electrons, are identified by the charge density difference between the negatively charged and the neutral systems, i.e., $f_+ = \Delta\rho_+ = \rho_{q(+1e)} - \rho_{q(0)}$. The nucleophilic sites, which are prone to donate electrons, are obtained through the charge density difference between the neutral and the positively charged systems, i.e., $f_- = \Delta\rho_- = \rho_{q(0)} - \rho_{q(-1e)}$. In the calculation of the Fukui functions, f_+ and f_-, the charge densities of the charged systems are obtained using the equilibrium geometries of the respective neutral systems. The electrophilic and nucleophilic sites of the pristine ZnO nanoparticle are shown in Fig. 1(b), and Fig. 1(c), respectively. From the analysis of Fig. 1(b) and (c), it is possible to conclude that the surface has six expressive amphoteric symmetric sites, located on the Zn atoms at the six corners of the octahedral ZnO nanoparticle. Thus, these six amphoteric sites will be considered as the preferable ones for the adsorption of organic ligands.

Fig.1: (a) ZnO nanocrystal model with 0.9 nm of diameter. The gray and red spheres represent the zinc and oxygen atoms, respectively. (b) Isosurface identifying the electrophilic f_+ and (c) the nucleophilic f_- sites of the ZnO nanocrystal.

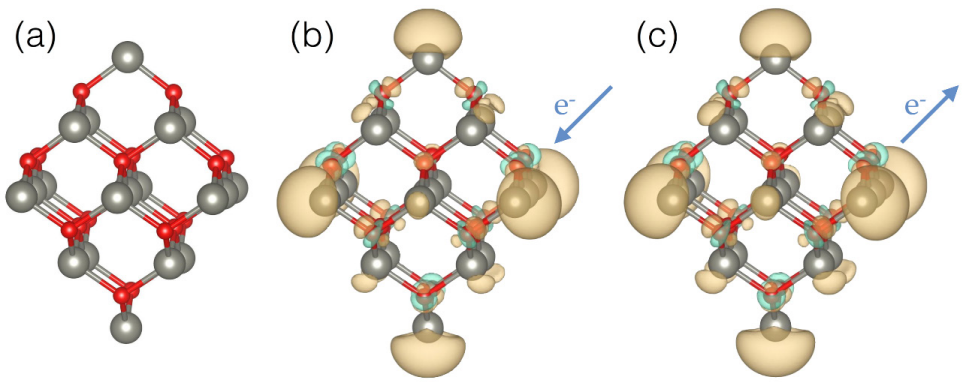

The thiol, amine, and phosphine groups are among the most common organic molecules used to cap semiconductor nanostructures, as ZnO nanocrystals (NCs) (GARCIA et al., 2007; VOZNYY, 2011). Representative molecules of these groups are dodecanethiol ($C_{12}H_{26}S$), dodecylamine ($C_{12}H_{27}N$) and trioctylphosphine (TOPO ($OP(C_8H_{17})_3$).

3.1 ORGANIC MOLECULES: THIOL, AMINE AND TOPO

In Fig. 2 (a), (b), and (c) the highest occupied (HOMO) and lowest unoccupied (LUMO) molecular orbitals are shown for each of these molecules. It can be observed that these frontier orbitals are located close to S, N and O atoms, respectively. These are the most probable regions to exchange electrons when these molecules act as functional agents. In order to reduce the computational efforts, the size of the hydrocarbon chains considered in the representative molecules has been reduced. The new representation of these molecules, now called simply as *thiol* (pentanethiol, $C_5H_{12}S$), *amine* (ethanamine, C_2H_7N), and *TOPO* ($OP(C_3H_7)_3$) as well as their respective frontier orbitals, are shown in Fig. 2(d), (e) and (f).

Fig.2: Structural model and the respective localization of HOMO and LUMO of representatives molecules of (a,d) thiol, (b,e) amine and (c,f) phosphine groups. The yellow, light blue, light purple, red, brown and light pink represents S, N, P, O, C and H atoms, respectively.

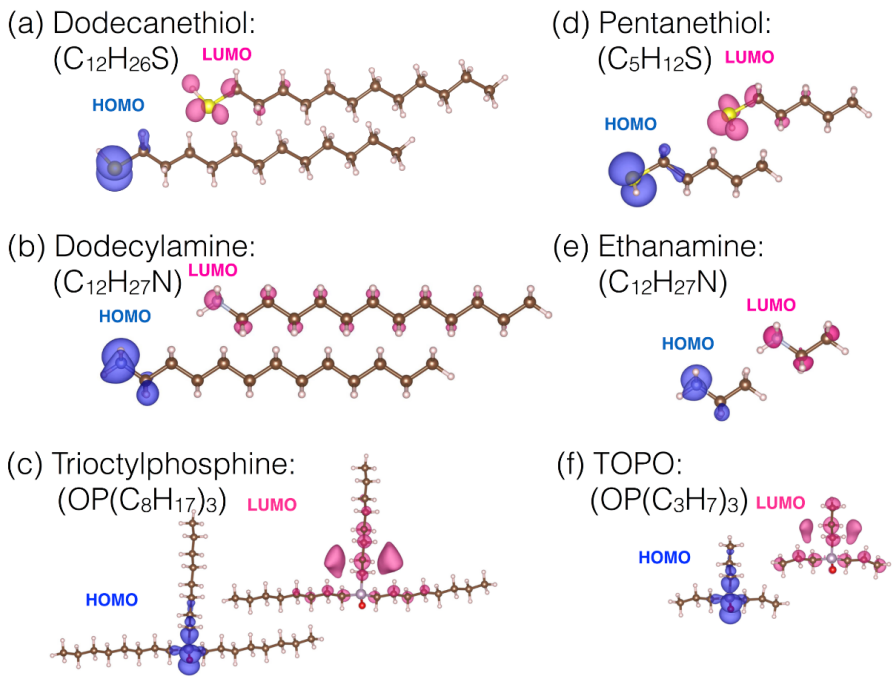

From Fig. 2 it is seen that, for the three considered molecules, the HOMO is more localized than the respective LUMO. Further, it is clear that the frontier orbitals are very similar to those for the molecules with longer hydrocarbon chains. This allows us to develop the investigation of ZnO NCs capped with thiol, amine and TOPO molecules while keeping the computational effort at a minimum.

3.2 STRUCTURAL PROPERTIES AND ENERGETICS

The results will be presented according to the number of ligands adsorbed on the ZnO NC. The studied models have one, two or six organic ligands, which will be connected to the reactive corners of the NC, as shown in Fig. 3. This allows to single-out the effects of the different number of ligands in the NC properties. Since all the reactive sites at the corners of the NC are symmetrically equivalent, the case of one adsorbed organic ligand implies in only one structural possibility. This is also true for the case of six adsorbed ligands, i.e., when there will be a ligand bonded to each reactive site in the NC. For two adsorbed ligands, there will be two non-equivalent structural possibilities: (*i*) when the ligands are bond to opposite sites, and (*ii*) when the ligands are at neighboring reactive sites in the NC. In this study, only the case (*i*) is considered.

Fig. 3: Representation of optimized ZnO NC capped with thiol, amine and TOPO molecules adsorbed in one, two or six amphoteric sites.

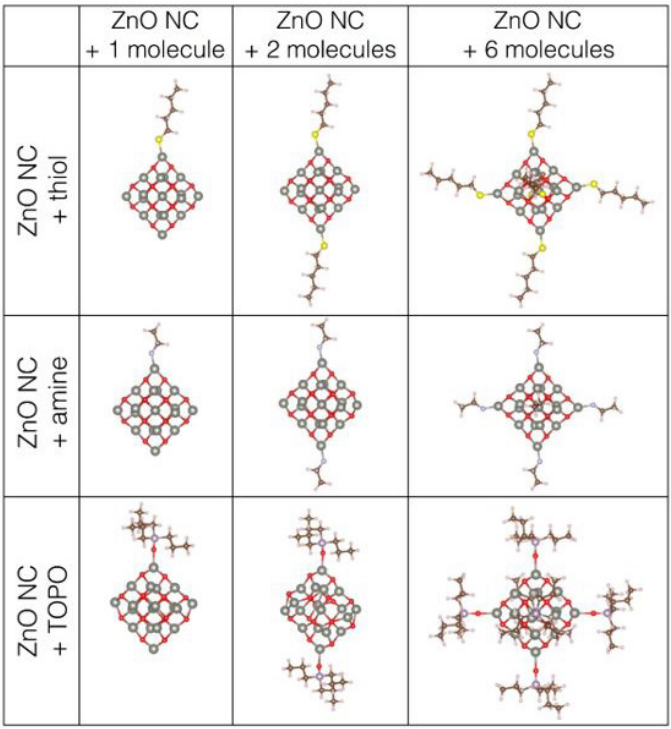

Fig. 4 presents the Zn-O bond length as a function of its distance from the center of ZnO NC. In the first column, it is possible to observe the behavior of the Zn-O bond length of the pristine NC with 35 atoms, i.e., without adsorbed molecules at its surface. It is clear from Fig. 4 that the NC has four crystalline Zn-O layers. Compared to the calculated zinc blende ZnO bulk (green dashed line), this NC has a small deviation (~ +0.05 Å) of its degenerated bond lengths at the two inner layers, while the bond lengths at the surface (the two outer layers) are very similar to those of the bulk (1.97 Å, PBE).

Fig. 4: Zn-O bond length as a function of the distance from the center of ZnO nanocrystal. The inset schemes represent ZnO NC (pale red sphere) with the different number of adsorbed thiol, amine and TOPO molecules (yellow, blue and violet rods, respectively).

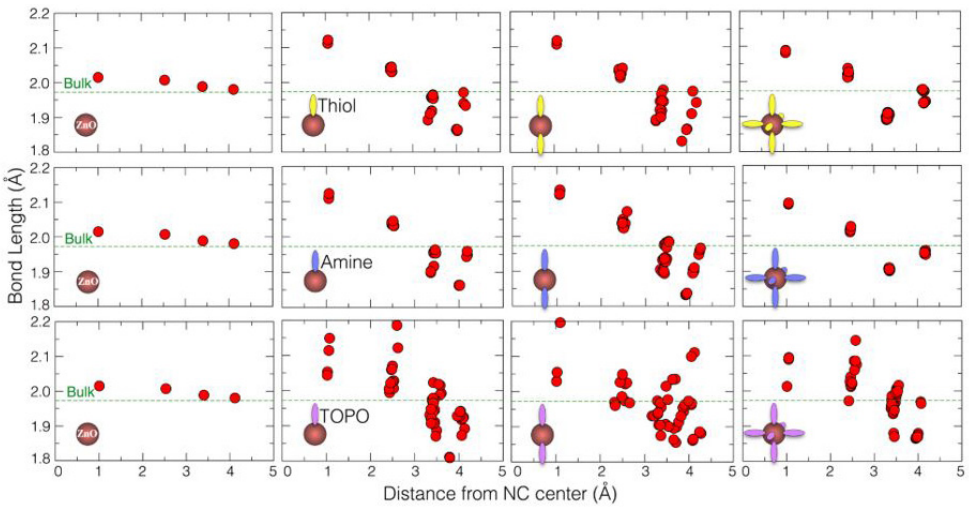

The first, second, and third rows represent the cases for thiol, amine and TOPO ligands, respectively. As expected, ZnO nanocrystal presents structural changes when molecules are adsorbed at its surface. The bond length variation within a layer reveals structural disorder and a break of the NC symmetry. The higher the variation the greater the distortion in the NC crystallinity induced by the adsorbed molecule. A common observation of the bond lengths is that, for all cases, greater values are observed in inner layers of the nanocrystal and shorter ones at the surface, regardless the adsorbed molecule or the number of capped sites. The Zn-O bond lengths suffer higher deviations (~ -0.17 Å to ~ +0.23 Å), as compared to the pristine ZnO NC. The Zn atom bonded to the organic molecule is pulled outward, compared to the pristine case, reaching distances circa 4.5 Å. This can also be identified through the angle O-Zn-O of this specific Zn atom. In the pristine case this angle is 130.1°, decreasing to 102.0°, 100.9°, and 124.5° when single molecules of thiol, amine and TOPO are adsorbed, respectively.

The second column in Fig. 4 represents the case of just one adsorbed molecule, and clearly shows that there is a more pronounced perturbation in the case of the TOPO molecule, where a Zn-O bond length variation is observed for all NC layers. For the cases where one thiol or one amine molecule is adsorbed, this perturbation is restricted to the external (or surface) layers, while the bond lengths in the internal layers remain degenerate.

In case of two TOPO adsorbed molecules, it is possible to observe a large structural deformation of the external layers, since it is not possible to clearly identify the crystalline pattern (layers of bonds), as shown in Fig. 3 and Fig. 4. When two thiol or amine molecules are adsorbed at NC, well defined layers can still be observed, although the dispersion in the bond lengths is greater than in the case of one adsorbed molecule. This loss of degeneracy is more pronounced in the external bonds, distant 2.5 Å or more from the NC center, reflecting the fact that the adsorbed molecules will perturb largely the atoms at the NC surface than those at the core.

When six molecules of thiol or amine are adsorbed to NC surface, i.e., when all the amphoteric sites are passivated, the symmetry of the system is partially recovered, presenting a less disturbed set of bond lengths in the surface. Furthermore, there are well defined layers of bonds, indicating a crystalline-like distribution, what can also be perceived in the structures of Fig. 3. In these cases, the external layer has bond lengths close to the bulk. For the case of the adsorption of six TOPO molecules, the crystalline symmetry is only partially recovered, having clearly defined layers, but presenting a variation of Zn-O bond lengths within each layer.

The distinct behavior of systems NC+TOPO is related to the different structural arrangement of this molecule: the thiol and amine molecules have a linear radical chain, while the TOPO presents a ramification in three linear radical chains. Since these chains have an umbrella-like conformation around the nanoparticle, their interaction with the NC will produce larger structural changes than thiol or amine molecules.

The adsorption energies (E_{ads}) presented in Table I are obtained for the charge-neutral nanostructured systems with one, two and six molecules adsorbed at the amphoteric sites. The E_{ads} are defined as:

$$E_{ads} = E_{ZnO+nX} - E_{ZnO} - E_{nX},$$

where E_{ZnO+nX} is the total energy of the ZnO NC with n adsorbed molecules, E_{ZnO} is the total energy of pristine ZnO NC, and E_{nX} is the total energy of nX molecules (X = thiol, amine or TOPO).

Table I: Adsorption energy (E_{ads}), charge transfer (C_T) and bond length average (d) for the ZnO+nX systems (X= thiol, amine or TOPO molecules). A positive C_T value indicates an electron transfer from the adsorbed molecules to ZnO NC.

System	% of capped sites	E_{ads}/molecule (eV)	C_T (e)	d (Å)
ZnO + 1 thiol	16	-3.20	-0.475	2.17
ZnO + 2 thiol	33	-3.22	-0.934	2.17
ZnO + 6 thiol	100	-3.16	-2.678	2.17
ZnO + 1 amine	16	-2.30	-0.555	1.86
ZnO + 2 amine	33	-2.29	-1.094	1.86
ZnO + 6 amine	100	-2.23	-3.175	1.86
ZnO + 1 TOPO	16	-1.97	0.125	1.97
ZnO + 2 TOPO	33	-1.63	0.298	1.99
ZnO + 6 TOPO	100	-0.93	0.183	2.04

The charge transfer C_T was calculated as the difference between the total charge of the nanoparticle with and without adsorbed molecules. The charge associated with each atom was obtained through the Bader charge analysis (HENKELMAN et al., 2006). Although the calculated charge transfer values can not to be directly compared with the experimental findings, they can give valuable information about the interactions between the NC and the thiol, amine, and TOPO molecules, as a function of the type and number of adsorbed molecules.

For one adsorbed thiol molecule (16% coverage of the amphoteric sites) the as-formed S-Zn bond length is 2.17 Å, which is lower than in the ZnS bulk (2.34 Å) (MADELUNG et al, 1982). For this case, the adsorption energy is -3.20 eV and the charge transfer from the ZnO nanoparticle to the thiol is 0.475 *e* (Table I). It is observed that, although being the ligand with the highest binding energy, the thiol molecule itself does not present severe structural changes. However, its adsorption can induce structural deformations at the surface and the inner structure of the nanoparticle. The same analysis is valid for the amine, with a N-Zn bond length of 1.86 Å. The adsorption energy of a single amine molecule is -2.30 eV, with a charge transfer of 0.555 *e* from the ZnO NP to the molecule. Although the larger bond length of S-Zn, as compared to N-Zn, the adsorption energies reveals a stronger interaction between the thiol molecule and the ZnO NC. The O-Zn bond distance is 1.97 Å, and the adsorption energy is -1.97 eV, with the TOPO being the weakly bonded molecule among those studied here. This is in agreement with previous results that showed that thiol has the strongest bond to semiconductor nanoparticles, with amine having intermediate values, and TOPO the weakest one (SPERLING et al.,

2010). This behavior is also valid for the charge transfer amount, being smaller for TOPO as compared to thiol and amine. It is observed from Table I that while thiol and amine act as electron acceptors, the TOPO molecule behaves as an electron donor. Previous studies suggest that, for low concentrations of TOPO in toluene, these molecules could behave as a Lewis base toward the semiconductor surface (LORENZ et al., 1998) which would explain the positive C_T values in Table I. When the number of adsorbed molecules at the surface increases, the adsorption energy per molecule decreases.

Considering the thiol, amine, and TOPO molecules interacting with the ZnO NC, it can be seen that the number if dangling bonds is one at the S atom, two at the N atom, and none at O. For each bond formed between the S or the N atoms and the ZnO NC, approximately half an electron will be transferred from the NC to thiol and amine molecules, respectively. These transferred charges will participate in (partially ionic) S-Zn and N-Zn bonds. This S-Zn chemical bond will saturate the S dangling bond. However, the N atom at the amine will remain with an unbounded electron. It will result in a net magnetic moment at the N atom. The O atom at the TOPO molecule, on the other hand, has no electrons to be shared, and the TOPO molecule is seen to donate electrons to ZnO NC, in agreement with the experimentally observed behavior (LORENZ et al., 1998).

3.3 ELECTRONIC PROPERTIES AND MAGNETIC PROPERTIES

The density of states (DOS) for the pristine nanocrystal is exhibited in Fig. 5, and can be considered as a reference for the cases where the interaction with external molecules is taken into account.

Fig. 5: Density of states (DOS, black line) of a pristine ZnO NC, obtained by a Gaussian convolution of σ = 0.01 eV of the individual energy levels (gray lines). The inset presents the structure with the correspondent plot of the spin density ($\Delta\rho = \rho\uparrow - \rho\downarrow$) isosurface in orange.

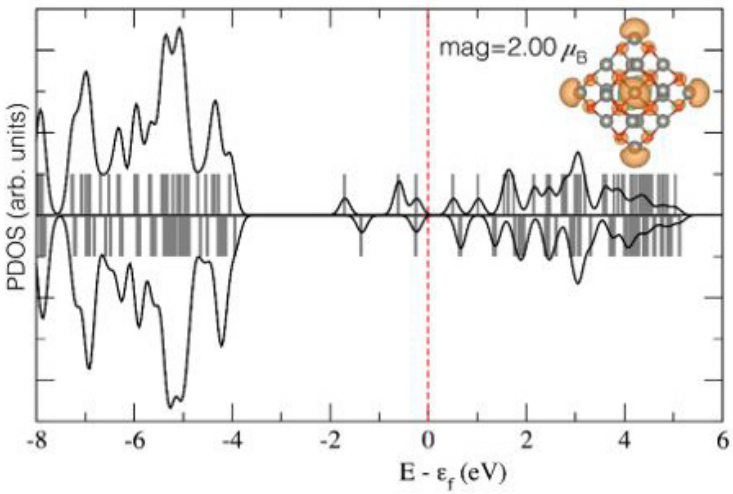

Fig. 6 and Fig. 7 show that the capping of the NC with any number of thiol and amine molecules results in energy levels close to the chemical potential, with contributions coming from both NC surface and adsorbed molecules. When the NC is capped with thiol molecules, the unpaired spin polarized electrons come from the NC, with no contribution from the molecule levels. On the other hand, for amine capped NCs, the spin polarized levels have contributions from both NC surface and the amine molecules.

Fig. 6: Density of states (DOS, black line) of ZnO NC, obtained by a Gaussian convolution of σ = 0.01 eV of the individual energy levels (gray lines), with (a) one, (b) two, and (c) six amphoteric sites functionalized by thiol molecules. The yellow lines are the PDOS on the thiol molecule(s). The right panels present structures with the correspondent plot of the spin density ($\Delta\rho$) isosurface in orange.

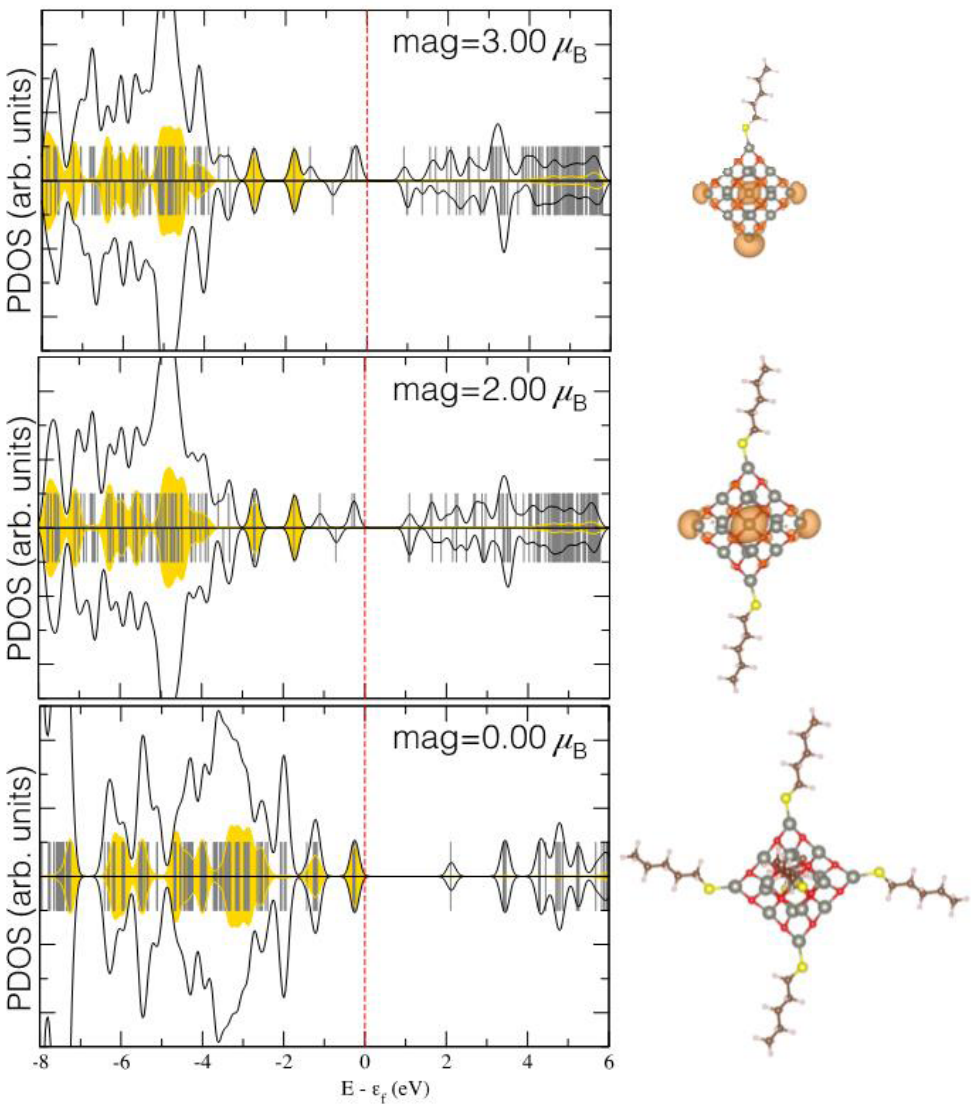

Fig. 7: Density of states (DOS, black line) of ZnO NC, obtained by a Gaussian convolution of σ = 0.01 eV of the individual energy levels (gray lines), with (a) one, (b) two, and (c) six amphoteric sites functionalized by amine molecules. The pale blue lines are the PDOS on the amine molecule(s). The right panels present structures with the correspondent plot of the spin density ($\Delta\rho$) isosurface in orange.

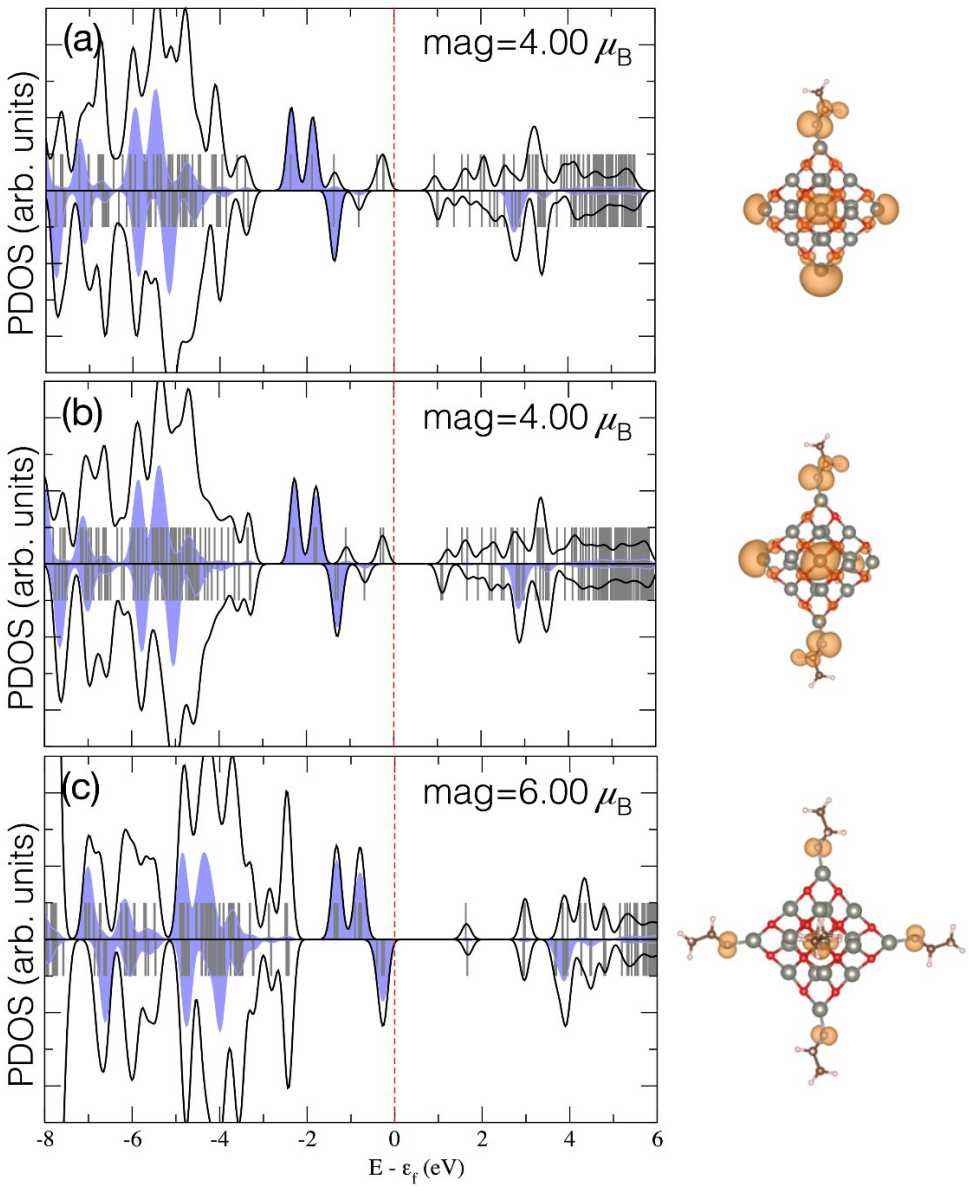

The PDOS at Fig. 8 shows that, contrarily to thiol and amine cases, the capping with TOPO molecules leads to levels close the chemical potential coming only from the NC, with the TOPO energy levels appearing deeper in energy. These results are in agreement with those reported by Garcia et al. (2007), who concludes that TOPO capped ZnO nanoparticles have an electronic configuration that is similar to the ZnO bulk.

The surface states at the corners of the pristine NC have a net magnetic moment. Five corners contribute with +0.5 μ_B and one with -0.5 μ_B, leading to a total magnetization of 2.0 μ_B. Similar results have been experimentally and theoretically reported for several nanostructured oxide semiconductors (PODILA, et al., 2010).

Fig. 8: Density of states (DOS, black line) of ZnO NC, obtained by a Gaussian convolution of σ = 0.01 eV of the individual energy levels (gray lines), with (a) one, (b) two, and (c) six amphoteric sites functionalized by TOPO molecules. The violet lines are the PDOS on the TOPO molecule(s). The right panels present structures with the correspondent plot of the spin density ($\Delta\rho$) isosurface in orange.

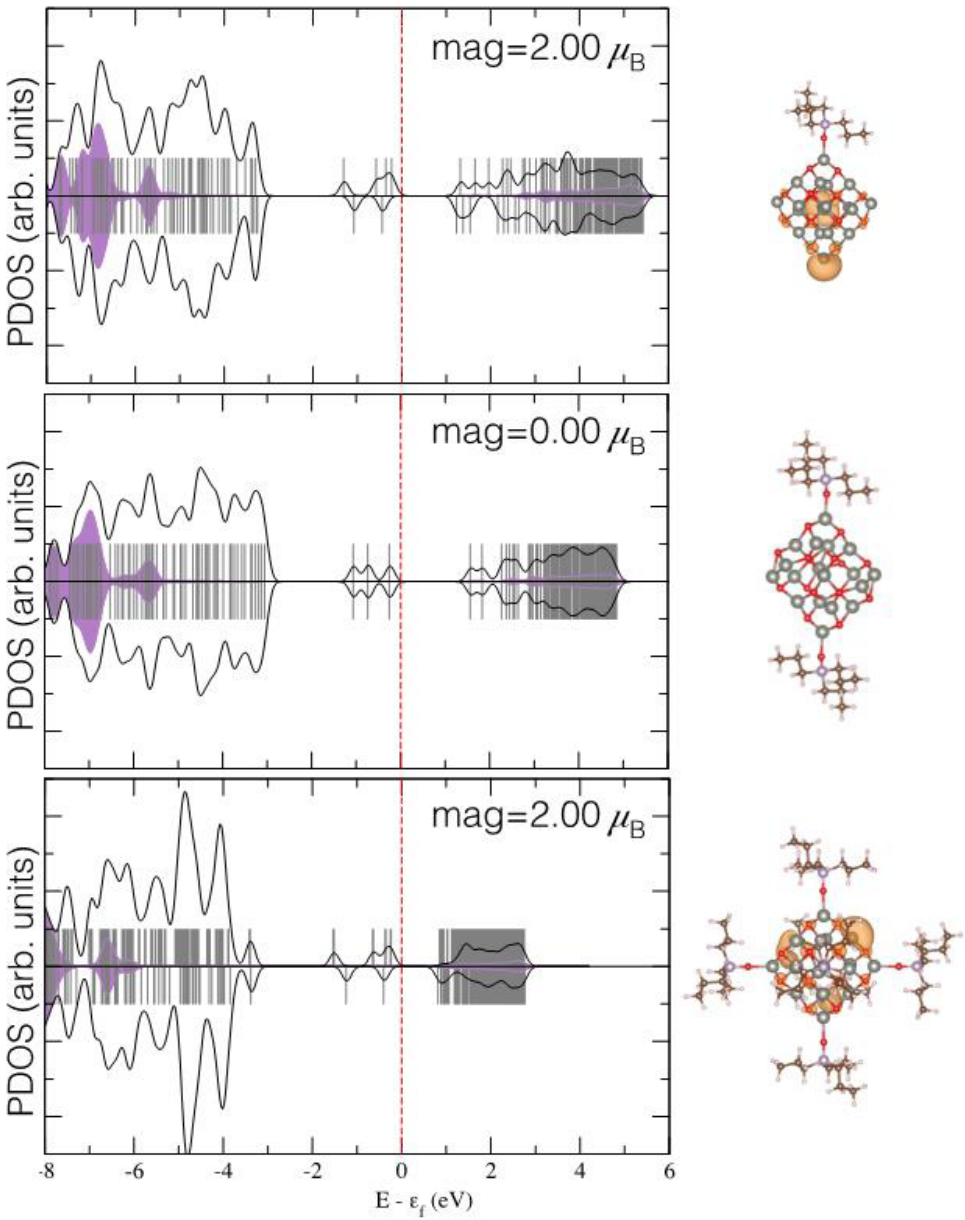

The partial passivation of the amphoteric sites from the pristine NC with thiol, amine, and TOPO functional groups results in highest occupied electronic levels (HOMO) that are singly-occupied and located at the NC surface. The spin polarization of the HOMO states can explain the magnetization of the capped ZnO NC. An exception to this behavior is observed for the case of the NC capped with two TOPO molecules. For this specific case, a large structural deformation of the two outermost layers is clearly seen in Fig. 4, leading to the vanishing of the localized surface magnetic moments.

It is interesting to observe that the total magnetization of the ZnO NC increases from 2.00 μ_B to 3.00 μ_B when one thiol molecule is adsorbed on its surface. It occurs due to a charge (spin) localization when the symmetry of the system is reduced, as a consequence of the interaction with one thiol molecule. Taking the corner where the thiol molecule is adsorbed as a reference, it is seen that the four first-neighbor corners have magnetic moments of 0.5 μ_B, while the opposite corner has 1.0 μ_B. When two thiol molecules are adsorbed at opposite sites of the NC, the total magnetization will be reduced from 3.00 μ_B to 2.00 μ_B. In the case of six thiol adsorbed molecules, the original ZnO NC symmetry is partially recovered, and the total magnetization is zero because all the reactive sites at the corners of NC are saturated.

Comparing Fig. 6 and Fig. 7, (a) and (b), it is observed that the magnetization of the NCs capped with one and two thiol and amine molecules differ by 1.00 μ_B and 2.00 μ_B, respectively. It is due to the resulting magnetic moments at the N atoms of the adsorbed amine molecules. The evidence of a localized magnetic moment of 1.00 μ_B at N atoms is made clearer when considering the NC capped with six thiols and six amine molecules. The total magnetization of the NC+6X systems is equal to 0.0 μ_B or X = thiol, and 6.0 μ_B for X = amine. Differently from the partial passivation with two thiol molecules, the magnetic moments for the case where two amine molecules are adsorbed will not be equally distributed among the remaining (four) unsaturated amphoteric sites. This happens because the interaction with two amine molecules induces greater structural changes at two of the unsaturated reactive sites, with a resulting spin concentration (1.0 μ_B) at the two structurally less perturbed sites, as can be seen in Fig. 7(b). It is important to point out that, in the case of amine, one electron will remain unpaired at the N atom, even after the N-Zn bonding is formed. This unpaired electron leads to net magnetic moments at the N atoms. Hence, if this dangling bond is saturated by, e.g., one H atom, the magnetic moments at the N atoms will vanish, which would probably lead to equal magnetizations for the ZnO NCs capped with the same number of thiol and amine molecules.

The interaction between the ZnO NC with TOPO molecules show a different behavior, as compared with those for thiol and amine cases. It has already been revealed

through the values of binding energies and charge transfers. The radical chains in the TOPO molecule are closer to the NC surface than those present at the thiol and amine molecules. This structural proximity will promote greater distortions in the NC external layers, as is clearly seen at Fig. 4. As already discussed, structural distortions lead to less symmetric structures and, consequently, to lower values of total magnetization.

For the case of one adsorbed TOPO molecule, three of the unsaturated corners will show greater deviations for the crystalline pattern, while two remaining corners showing structures that are more similar to those at the pristine NC. This leads to a concentration of the spin density on these two less disturbed corners, each one with a magnetic moment of 1.0 μ_B. The adsorption of two TOPO molecules induces structural distortions of the two outer layers of the NC, as shown in Fig. 4. This leads to a total magnetization equal to zero. It shows that the maintenance of the crystalline structural pattern is important for the spin density concentration and a resulting magnetization of the system. When six TOPO molecules are adsorbed by the NC, the structural ordering of the outer two layers of the NC is partially recovered (see Fig. 4). As a consequence, a net magnetization of 2.0 μ_B is obtained. However, the spin density on the NC surface has no defined pattern, showing a random distribution.

This direct relationship between the surface structural distortion of the capped NCs and its resulting magnetization is in agreement with experimental findings of Garcia et al., which measured the magnetic responses of pristine ZnO NCs capped with thiol, amine and TOPO molecules. The authors show that the magnetization magnitudes of the capped NCs show the following order: thiol capped NC > amine capped NC > TOPO capped NC. As has been pointed out, the thiol capped ZnO NCs have the lowest structural distortions, and the TOPO capped NCs the largest. The amine capped NC exhibiting intermediate surface structural distortions.

4 CONCLUSIONS

In conclusion, first principles DFT calculations have been used to systematically investigate the structural, electronic, energetic and magnetic properties of nX-capped ZnO nanocrystals (n is the number of molecules, X = thiol, amine or TOPO). When capped with thiol and amine molecules, a charge transfer from the ZnO NC to the adsorbed molecules is determined, and strong (partially ionic) chemical bonds are formed. On the other hand, a relatively weak bond is observed between the TOPO molecule and the NC, with electrons being transferred from TOPO to the NC. The valence states close to the chemical potential show contributions from both the NC and the organic molecules for the NC+thiol and

NC+amine systems. However, only the NC contributes to the levels close to the chemical potential for the NC+TOPO compound. The structural distortions appearing at the surface layers of the NC, due to the interactions with the organic molecules, are larger for TOPO than for amine, while are lower for thiol molecules. The resulting magnetization of these NC+molecules systems is seen to be related to the level of structural distortions of the NC surface layers as well as the saturation of the active adsorption sites at the NC surface, with greater magnetic moments for thiol and amine than for TOPO. These results provide atomistic explanations for the puzzling experimental findings, relating the structural and the magnetic properties of these oxides with their resulting magnetic moments.

5 ACKNOWLEDGMENTS

This study was financed by the Coordenação de Aperfeiçoamento de Pessoal de Nível Superior – Brasil (CAPES) – Finance Code 001. P. C. P. is thankful to the Conselho Nacional de Desenvolvimento Científicio e Tecnológico - CNPq - Grant n° 312388/2018-7. The Calculations were performed using the Brazilian computational facilities of CENAPAD/Campinas, and CPAD/UFSM.

REFERENCES

ADAMO, C.; BARONE, V. **Toward reliable density functional methods without adjustable parameters: The PBE0 model**. J. Chem. Phys., 1999, v. 110, p. 6158.

ALLISON, T. C.; TONG, Y. J. **Application of the condensed Fukui function to predict reactivity in core-shell transition metal nanoparticles.** Electrochimica Acta, 2013, v. 101, p. 334.

AZPIROZ, Jon M.; DE ANGELIS, Filippo. **Ligand Induced Spectral Changes in CdSe Quantum Dots**. ACS Appl. Mater. Interfaces, 2015, v. 7, p. 19736.

BHATTACHARYA, S. Kr.; KSHIRSAGAR A. **First principle study of free and surface terminated CdTe nanoparticles.** Eur. Phys. J. D., 2008, v. 48, p. 355.

BLOCHL, P. E. **Projector Augmented-Wave Method**. Phys. Rev. B, 1994, v. 50, p. 17953.

BOUOUDINA, M. et al. **Structural and magnetic properties and DFT analysis of ZnO:(Al,Er) nanoparticles.** RSC Adv., 2017, v. 7, p. 32931.

CHABAN, V. V.; PREZHDO, V. V.; PREZHDO, O. V. **Covalent Linking Greatly Enhances Photoinduced Electron Transfer in Fullerene-Quantum Dot Nanocomposites: Time-Domain Ab Initio Study.** J. Phys. Chem. Lett., 2013, v. 4, p. 1.

CHEN, J. et al. **Ultrafast Photoinduced Interfacial Proton Coupled Electron Transfer from CdSe Quantum Dots to 4,4-Bipyridine.** J. Am. Chem. Soc., 2016, v. 138, p. 884.

GAO, S. et al. **Creation of passivated Nb/N p-n co-doped ZnO nanoparticles and their enhanced photocatalytic performance under visible light illumination.** J. Mater. Sci. Technol., 2019, v. 35, p. 610.

GARCIA, M. A. et al. **Magnetic Properties of ZnO Nanoparticles.** Nano Letters, 2007, v. 7, p. 1489.

GHOUL, J. El; AL HARBI, F. F. **Synthesis, structural, optical and magnetic properties of Gd co-doped ZnO:V nanoparticles**. Solid State Commun., 2020, v. 314, p. 113916.

GUGLIERI, C. et al. **XMCD Proof of Ferromagnetic Behavior in ZnO Nanoparticles.** J. Phys. Chem. C, 2012, v. 116, p. 6608.

HENKELMAN G.; ARNALDSSON, A.; JONSSON, H. **A fast and robust algorithm for Bader decomposition of charge density**. Comput. Mater. Sci., 2006, v. 36, p. 254.

HINES, Douglas A.; KAMAT, Prashant V. **Recent Advances in Quantum Dot Surface Chemistry**. ACS Appl. Mater. Interfaces, 2014, v.6, p. 3041.

HOHENBERG, P.; KOHN, W. **Inhomogeneous Electron Gas**. Phys. Rev., 1964, v. 136, p. B864.

KANGOA, S. et al. **Surface modification of inorganic nanoparticles for development of organic-inorganic nanocomposites: A review**. Progress in Polymer Science, 2013, v. 38, p. 1232.

KIM, S. et al. **Type-II Quantum Dots: CdTe/CdSe(Core/Shell) and CdSe/ZnTe (Core/Shell) Heterostructures.** J. Am. Chem. Soc., 2003, v. 125, p. 11466.

KITTILSTVED, K. R.; GAMELIN, D. R. **Activation of High-TC Ferromagnetism in Mn2+-Doped ZnO using Amines**. J. Am. Chem. Soc., 2005, v. 127, p. 5292.

KOPPING, J. T.; PATTEN, T. E. **Identification of Acidic Phosphorus-Containing Ligands Involved in the Surface Chemistry of CdSe Nanoparticles Prepared in Tri-N-octylphosphine Oxide Solvents.** J. Am. Chem. Soc., 2008, v. 130, p. 5689.

KRESSE, G.; FURTHMULLER, J. Efficient iterative schemes for ab initio total-energy calculations using a plane-wave basis set. Phys. Rev. B, 1996, v. 54, p. 11169.

KUZNETSOV, Aleksey E.; BERATAN, David N. Structural and Electronic Properties of Bare and Capped $Cd_{33}Se_{33}$ and $Cd_{33}Te_{33}$ Quantum Dots. J. Phys. Chem. C, 2014, v. 118, p. 7094.

LORENZ, J. K.; ELLIS, A. B. **Surfactant-Semiconductor Interfaces: Perturbation of the Photoluminescence of Bulk Cadmium Selenide by Adsorption of Tri-n-octylphosphine Oxide as a Probe of Solution Aggregation with Relevance to Nanocrystal Stabilization.** J. Am. Chem. Soc., 1998, v. 120, p. 10970.

MADELUNG, O.; SCHULZ, M.; WEISS, H. **Semiconductors, Physics of Group IV Elements and III-V Compounds.** New Series, Group III. New York: Springer-Verlag, 1982, v. 17.

NOH, K. et al. **Effect of ethanolamine passivation of ZnO nanoparticles in quantum dot light emitting diode structure**. Curr. Appl. Phys., 2019, v. 19, p. 998.

OSORIO-GUILLEN, J. et al. **Magnetism without Magnetic Ions: Percolation, Exchange, and Formation Energies of Magnetism-Promoting Intrinsic Defects in CaO.** Phys. Rev. Lett., 2006, v. 96, p. 107203.

PARK, Y.; FELIPE, M. J.; ADVINCULA, R. C. **Facile Patterning of Hybrid CdSe Nanoparticle Films by Photoinduced Surface Defects**. ACS Appl. Mater. INTERFACES, 2011, v. 3, p. 4363.

PARR, Robert G.; YANG, Weitao. **Density-Functional Theory of Atoms and Molecules**. Oxford: Oxford University Press, 1989.

PERDEW, J. P.; BURKE, K.; ERNZERHOF, M. **Generalized Gradient Approximation Made Simple.** Phys. Rev. Lett., 1997, v. 77, p. 3865.

PODILA, R. et al. **Origin of FM Ordering in Pristine Micro- and Nanostructured ZnO**. Nano Letters, 2010, v. 10, p. 1383.

SAMANTA, A.; GOSWAMI, M. N.; MAHAPATRA, P. K. **Magnetic and electric properties of Ni-doped ZnO nanoparticles exhibit diluted magnetic semiconductor in nature.** J. Alloy Compd., 2018, v. 730, p. 399.

SCHOENHALZ, A. L. et al. **Surface magnetization in non-doped ZnO nanostructures.** Appl. Phys. Lett., 2009, v. 94, p. 162503.

SINGLA, M. L.; SHAFEEQ M., M.; KUMAR, M. **Optical characterization of ZnO nanoparticles capped with various surfactants**. Journal of Luminescence, 2009, v. 129, p. 434.

SPERLING, R. A.; PARAK, W. J. **Surface modification, functionalization and bioconjugation of colloidal inorganic nanoparticles**. Phil. Trans. R. Soc. A, 2010, v. 368, p. 1333.

TALAPIN, D. V. et al. **Highly Luminescent Monodisperse CdSe and CdSe/ZnS Nanocrystals Synthesized in a Hexadecylamine-Trioctylphosphine Oxide-Trioctylphospine Mixture.** Nano Letters, 2001, v. 1, p. 207.

TANG, Y. et al. **Geometric stability, electronic structure, and intercalation mechanism of Co adatom anchors on graphene sheets.** J. Phys.: Condens. Matter, 2015, v. 27, p. 255009.

TSUI, E. Y.; HARTSTEIN, K. H.; GAMELIN, D. R. **Selenium Redox Reactivity on Colloidal CdSe Quantum Dot Surfaces.** J. Am. Chem. Soc., 2016, v. 138, p. 11105.

VOZNYY, Oleksandr. **Mobile Surface Traps in CdSe Nanocrystals with Carboxylic Acid Ligands.** J. Phys. Chem. C, 2011, v. 115, p. 15927.

WANG, Jing; HAN, Heyou. **Hydrothermal synthesis of high-quality type-II CdTe/CdSe quantum dots with near-infrared fluorescence**. Journal of Colloid and Interface Science, 2010, v. 351, p. 83.

WUISTER, S. F.; DONEGA, C. M.; MEIJERINK, A. **Influence of Thiol Capping on the Exciton Luminescence and Decay Kinetics of CdTe and CdSe Quantum Dots**. J. Phys. Chem. B, 2004, v. 108, p. 17393.

YU, M. et al. **First principles study of CdSe quantum dots: Stability, surface unsaturations, and experimental validation**. Appl. Phys. Lett., 2006, v. 88, p. 231910.

YU, X.-f. et al. **Monolayer Ti_2CO_2: A Promising Candidate for NH_3 Sensor or Capturer with High Sensitivity and Selectivity**. ACS Appl. Mater. Interfaces, 2015, v. 7, p. 13707.

ZHU, H. et al. **Synthesis and Optical Properties of Thiol Functionalized CdSe/ZnS (Core/Shell) Quantum Dots by Ligand Exchange.** J. Nanomater., 2014, v. 2014, p. 324972.

ABOUT THE ORGANIZER

MARCOS AUGUSTO DE LIMA NOBRE: Assistant Professor and Researcher (2006 - present), with citation name M. A. L. Nobre, at the São Paulo State University (UNESP), School of Science and Technology, Department of Physics, campus at Presidente Prudente-SP. Head and Founder (2002) of the Laboratory of Functional Composites and Ceramics (LaCCeF acronym in Portuguese, the native idiom), Lab certified by PROPE-UNESP/National Council for Scientific and Technological Development/CNPq*. Grants from National Council for Scientific and Technological Development (CNPq), 2020-2023, 2019-2021 and 2010-2012. Granted with Young-Researcher scholarship by the São Paulo Research Foundation, FAPESP (São Paulo, São Paulo) (2002 - Summer of 2005). Postdoctoral fellow at the Polytechnic School of the University of Sao Paulo (POLI USP-SP) Metallurgy and Materials Science Department with FAPESP Scholarship (1999-summer of 2000). PhD in Science, CAPES Scholarship (Physical Chemistry 1999) by the Chemistry Department, UFSCar-SP. Master in Chemistry CNPq scholarship (Physical Chemistry 1995) by the Chemistry Department, UFSCar-SP. Licentiate degree (4-year of study) in Physics (1993) CNPq and CNPq-Rhae scholarships by the Physics Department, UFSCar-SP. Associate Editor of the Micro & Nano Letters - IET 2019-2020. Associate Editor of the Micro & Nano Letters-Wiley, 2020 - present. Ethycal Editor of the Applied Mathematics Science (Reuse) m-Hikari and Modern Research in Catalysis, Irvine-CA, USA (2017- date). Editorial board member of the Artemis Editora, Brazil. Nowadays, have 02 patents. Has published 80 papers at 39 different indexed Journals of renowned Editors. In May/25/2021, has been cited 1379 times, at 76 papers (47 with citations), in according to the ResearchID actual Publons base having an H-index equal to 23. Academic Google score: H = 28, i10 = 45 and 2338 citations. Reviewer of more than three dozen of journals. Have more than 580 communications and presentation in National and International Congress and Symposiums, from these 150 has been published as Conference Paper. Author or co-author of 20 Chapters of book approaching Scientific Divulgation, Teaching of Physic and Chemistry for teachers actuating in the graduating degree. For this, the Nanoscience and Nanotechnology have been the first strategy. Received tens of National and International Awards, Honorable mentions and distinction mentions, as well as titles. Research skills: Materials Science, Advanced Ceramic Processing, Linear and Non-linear Advanced Dielectrics Materials, Solid state chemistry, Impedance spectroscopy of solids and fluids, Structural Characterization via Mid infrared Spectroscopy with Fast-Fourier-Transformed of solid and fluids, Structural and non-structural Phase Transitions in Semiconductor Ferroelectrics. Also, Molecular Interactions in Functional Fluids as biofuels and its blends, probed via mid infrared Spectroscopy. Research interests: New Functional Materials as

amorphous composite based on carbon/nanoparticles and Semiconductor Ferroelectrics. Member of the Program of Post-Graduation in Chemistry at UNESP - Campus of São José do Rio Preto, IBILCE UNESP – SP, Brazil.

INDEX

G

K

M

N

O

Z

EDITORA
ARTEMIS